PERGAMON

Carbon 41 (2003) 2573–2584

CARBON

Preparation and characterization of trilobal activated carbon fibers

Young-Seak Lee[a,b], Yulia V. Basova[b], Dan D. Edie[b,*], Laura K. Reid[b], Steven R. Newcombe[b], Seung-Kon Ryu[c]

[a]*Department of Chemical Engineering, Nanotechnology Center, Sunchon National University, Sunchon 540-742, South Korea*
[b]*Center for Advanced Engineering Fibers and Films, 301 Rhodes Hall, Clemson University, Clemson, SC 29634-0910, USA*
[c]*Department of Chemical Engineering, Chungnam National University, Daejeon 307-764, South Korea*

Received 4 April 2003; accepted 14 July 2003

Abstract

The objective of this research was to evaluate the effectiveness of several different methods for controlling the pore size and pore size distribution in activated carbon fibers. Variables studied included fiber shape, activation time, and the addition of small amounts of silver nitrate. Pure isotropic pitch and the same isotropic pitch containing 1 wt.% silver were melt spun to form fibers with round and trilobal cross sections. These fibers were then stabilized, carbonized, and activated in carbon dioxide. Field emission scanning electron microscopy (FE SEM), electron dispersive spectra (EDS), and wavelength dispersive spectra (WDS) were used to monitor the size and distribution of the silver particles in the fibers before and after activation. Each of these analyses showed that the distribution of silver particles was extremely uniform before and after activation. The fibers were also weighed before and after activation to determine the percent burn-off. The BET specific surface areas of the activated fibers were determined from N_2 adsorption isotherms measured at $-196\,^{\circ}C$. The results showed that round and trilobal fibers with equivalent cross-sectional areas yielded similar burn-off values and specific surface areas after activation. Also, activation rates were found to be independent of CO_2 flow rate. The porosity of the activated fibers depended on the total time of activation and the cross-sectional area of fibers. The N_2 adsorption measurements showed that the activated fibers had extremely high specific surface areas (greater than 3000 m^2/g) and high degrees of meso- and macro-porosity. FE SEM was also used to investigate surface texture and size of pore openings on the surfaces of the activated fibers. The photos showed that silver particles generated surface macro- and mesopores, in agreement with the inferences from N_2 adsorption measurements.

Keywords: A. Carbon fibers; B. Mixing; Activation; C. BET surface area; D. Porosity

1. Introduction

Activated carbon fibers (ACFs) have attracted considerable attention because of their high adsorption rates and capacities, their ease of synthesis in various forms, and their wide applicability for purification, separation or catalysis. Currently, ACFs are produced by subjecting a fibrous material, formed from a PAN, rayon, phenolic resin, or pitch precursor, to a carbonization/activation process. This creates pores with an average diameter of about 10 Å (micropores), giving the fibers specific surface areas of over 2000 m^2/g. Although these ACFs have many attractive properties, fibers with larger pore diameters (mesopores) are needed to separate larger molecules such as proteins and humin fractions, as well as pollutants and many pesticides.

The goal of this work is to develop ACFs with pore sizes and pore size distributions designed to efficiently adsorb specific toxins. A secondary goal is to develop ACFs that generate very little pressure drop in filter applications. These two improvements could significantly increase the efficiency of ACFs and simplify the design of sorption processes for environmental pollution control. ACFs containing uniform mesoporosity could also prove

*Corresponding author. Tel.: +1-864-656-4535; fax: +1-864-656-0784.
E-mail address: dan.edie@ces.clemson.edu (D.D. Edie).

0008-6223/03/$ – see front matter
doi:10.1016/S0008-6223(03)00376-2

valuable in other applications, such as catalysis and electronics.

Previous researchers have added compounds containing metals such as Ag, Co, Cu, Y and Al to polymeric and isotropic pitch precursors, formed these precursors into ACFs, and then measured their adsorption characteristics [1–7]. While these studies have shown that the metal additives can generate mesopores during activation, the attainment of a uniform distribution of these metals in the precursors has been a problem. Often the metals appear to coalesce during activation, leading to a wide variation in pore sizes.

In this paper, a new approach was developed for dispersing metal compounds in isotropic pitch. Samples of the metal-containing isotropic pitch prepared by this technique, as well as samples of the pure isotropic pitch, were melt spun into carbon fibers with round and trilobal cross sections. These fibers were then stabilized, carbonized, and activated in carbon dioxide. Finally, the structural properties and specific surface areas of the ACFs were compared to estimate the effect of metal additives and fiber shape on the production process and the final porosity.

2. Experimental

2.1. Materials

The spinnable isotropic pitch was prepared by the two-stage thermal condensation of a naphtha cracking bottom (NCB) oil supplied by the SK Oil Refinery Company in Korea. The procedure involved heating about 4 kg NCB oil from room temperature to 360 °C at a heating rate of 2 °C/min under a nitrogen flow of 3 l/min and then held the pitch at this temperature for 3 h. The pitch was cooled to 330 °C and then reheated to 360 °C. The pitch was held at this temperature for an additional 3 h. The properties of the naphtha cracking bottom oil and reformed pitch used in the present work are summarized in Table 1. The softening point was measured using a Mettler FP 800 (USA).

2.2. Preparation of pitch–silver nitrate ($AgNO_3$) mixtures

Silver nitrate powder (m.p. 212 °C) was directly mixed into reformed pitch to prepare precursor pitch containing 1.0 wt.% of silver. In order to get a homogenous dispersion of the silver, the silver nitrate was first ground into particles with an average size of 100 nm. These solid particles were then loaded into an intensive mixer (Thermo Haake, Rheomix) with an appropriate amount of isotropic pitch particles to yield a mixture containing 1.0 wt.% silver. Next, the mixing chamber was sealed and continuously purged with nitrogen. The chamber was then heated to 10 °C below the softening point of the isotropic pitch. Once the temperature had reached steady-state, the drive motor was energized. The motor drives the mixer's two opposing rotors at a controlled, preset rate. Dispersive mixing takes place in the high shear zone between these rotors and the walls of the mixing chamber. An air-cooling system prevents temperature overshoot due to frictional heat. Finally, after a preset time, the motor was stopped and the heaters turned off. After the mixture cooled to room temperature, it was ground into a fine homogeneous powder using a mortar and pestle and stored in sealed glass bottles.

2.3. Melt spinning

The pure isotropic pitch and the pitch–$AgNO_3$ mixture were melt spun into round (R) and trilobal (T) fibers using a batch extrusion system. A brief description of the apparatus is given here, and additional details can be found elsewhere [8,9]. This extruder uses a positive-displacement gear drive, which fixes the flow rate [9]. A spinneret with 12 150-μm-diameter capillaries was attached to the bottom of a stainless steel cartridge to produce multifilament tows of fibers with circular cross sections. A second spinneret containing 12 holes with trilobal cross sections was used if trilobal fibers were desired. After the spinneret was attached, pitch powder was loaded into the cartridge. Then a piston was placed in the top of the cartridge to compress the pitch. A wire mesh filter (50 μm) was inserted prior to the spinneret to ensure uniform mixing and distribution of pitch, thus enhancing spinnability. The cartridge and piston were placed in the heating section of the extruder and brought to the desired spinning temperature. The take-up speed of the fibers was controlled so that the desired diameter was achieved. The winding speed was constant for each trial.

Table 1
Properties of naphtha cracking bottom (NCB) oil and reformed isotropic pitch

Pitches	Softening point (°C)	Elemental analysis (wt.%)			Solubility (wt.%)[a]			Aromatic ratio (C/H)
		C	H	N	BI	QI	HI	
NCB	–	90.2	6.9	0.1	[b]	0.05	[b]	1.1
Isotropic	250	90	5	[b]	39	0.62	95.1	1.5

[a] BI, benzene-insoluble; QI, quinoline-insoluble; HI, hexane-insoluble fractions.
[b] None detected.

2.4. Stabilization and carbonization

As-spun fibers were cut into about 5-cm bundles weighing ~0.5 g and placed into a forced-convection oven, supplied by Fisher Scientific (USA). The fiber bundles were then heated in air at 0.5 °C/min to 265 °C and held at this temperature for 13–15 h. Previous studies had shown that this results in an 8 to 10% weight gain, a good indication that the fiber sample is fully stabilized [10]. To monitor the weight gained during the stabilization, the fibers were weighed before and after the stabilization process. The stabilized fiber sets were then placed in a graphite-paper boat and placed in an Astro graphite resistance furnace. The furnace was purged with industrial grade helium. All fiber samples were heated at a rate of 10 °C/min to 1000 °C and then held at this temperature for 1 h.

2.5. Preparation of activated carbon fibers (ACFs)

Finally, the carbon fiber sets were activated using a temperature-controlled tube furnace. Prior to activation, the carbon fibers were pre-heated in flowing CO_2 for 30 min. Activation consisted of exposing the fibers to pure CO_2 at atmospheric pressure and 900 °C for times ranging from 10 to 360 min. The CO_2 flow rates were maintained at either 0.25 or 0.5 l/min. The fiber samples were weighed before and after activation to determine the percent mass change, termed burn-off (BO).

2.6. Characterization

Cross sections and surfaces of as-spun, carbonized, and activated carbon fibers were inspected by field emission scanning electron microscopy (FE SEM), electron dispersive spectra (EDS), and wavelength dispersive spectra (WDS) to monitor the distribution of silver particles after each step of the process. The chemical composition of the metal-containing fibers before and after activation was determined by analyzing cross sections and fiber surfaces by EDAX connected to a Hitachi 3500 SEM (Japan).

To qualitatively examine the texture of the circular and trilobal-shape ACFs, representative samples of the fibers were cut into ~0.5 cm lengths, attached with carbon tape to aluminum stubs, and examined using a Hitachi FE SEM 4700, in the secondary electron mode and a Hitachi 3500 SEM in the back scattering mode.

The adsorption characteristics of the ACFs were determined by generating N_2 adsorption isotherms at −196 °C using a Coulter SA 3100 apparatus (USA). A Micromeritics 2020 instrument was used to measure nitrogen adsorption isotherms at −196 °C between relative pressures of 5×10^{-7} and 1. The same instrument was also

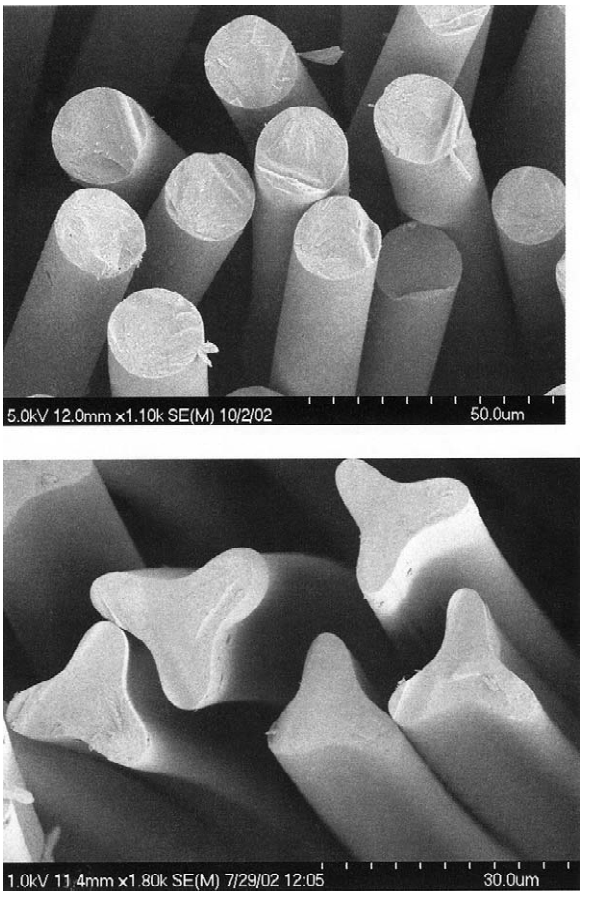

Fig. 1. FE SEMs of cross sections of round and trilobal carbon fibers melt spun from isotropic pitch containing 1% silver nitrate.

Table 2
Melt-spinning conditions for round fibers and trilobal fibers using the pure isotropic pitch and the silver-containing isotropic pitch

Fiber shape	Round						Trilobal					
	Unmixed			Mixed			Unmixed			Mixed		
	(1)[a]	(2)[a]	(3)[a]	(1)	(2)	(3)	(1)	(2)	(3)	(1)	(2)	(3)
Spinning yields (%), >	83	75	75	54	50	42	65	58	54	33	25	16
Spinning temperatures (°C)	270–272			276–280			263–267			265–270		

[a] The numerical notations indicate the relative takeup speeds: (1) 286 m/min, (2) 457 m/min, (3) 640 m/min.

Table 3
Diameters of as-spun and carbonized round fibers

Fibers	*d*, μm (as-spun)	*d*, μm (carbonized)
KUR1	19.2–22.8	18.1–21.0
KUR2	16.0–20.6	15.6–18.4
KUR3	13.8–15.5	13.1–14.9
KMR1	12.3–18.0	11.6–16.8
KMR2	11.2–18.6	10.1–15.5
KMR3	10.7–15.2	8.2–12.7

used to measure adsorption/desorption isotherms on selected samples. All samples were outgassed at 330 °C for 3 h prior to each adsorption experiment.

3. Results and discussion

3.1. Melt spinning pure and silver-containing pitches through spinnerets with multiple holes

The spinning temperatures and average yields for the melt spinning of both the pure isotropic and silver-containing pitches are given in Table 2. The spinning yield is defined as the total mass of the fibers collected during the spinning trial divided by the mass of the pitch that had been loaded into the cartridge prior to the trial times 100%. As shown in Table 2, the spinning yields were quite good for the round fibers produced from the pure (unmixed) and mixed isotropic pitch precursors. Nevertheless, the pure precursor samples were easier to melt spin than the

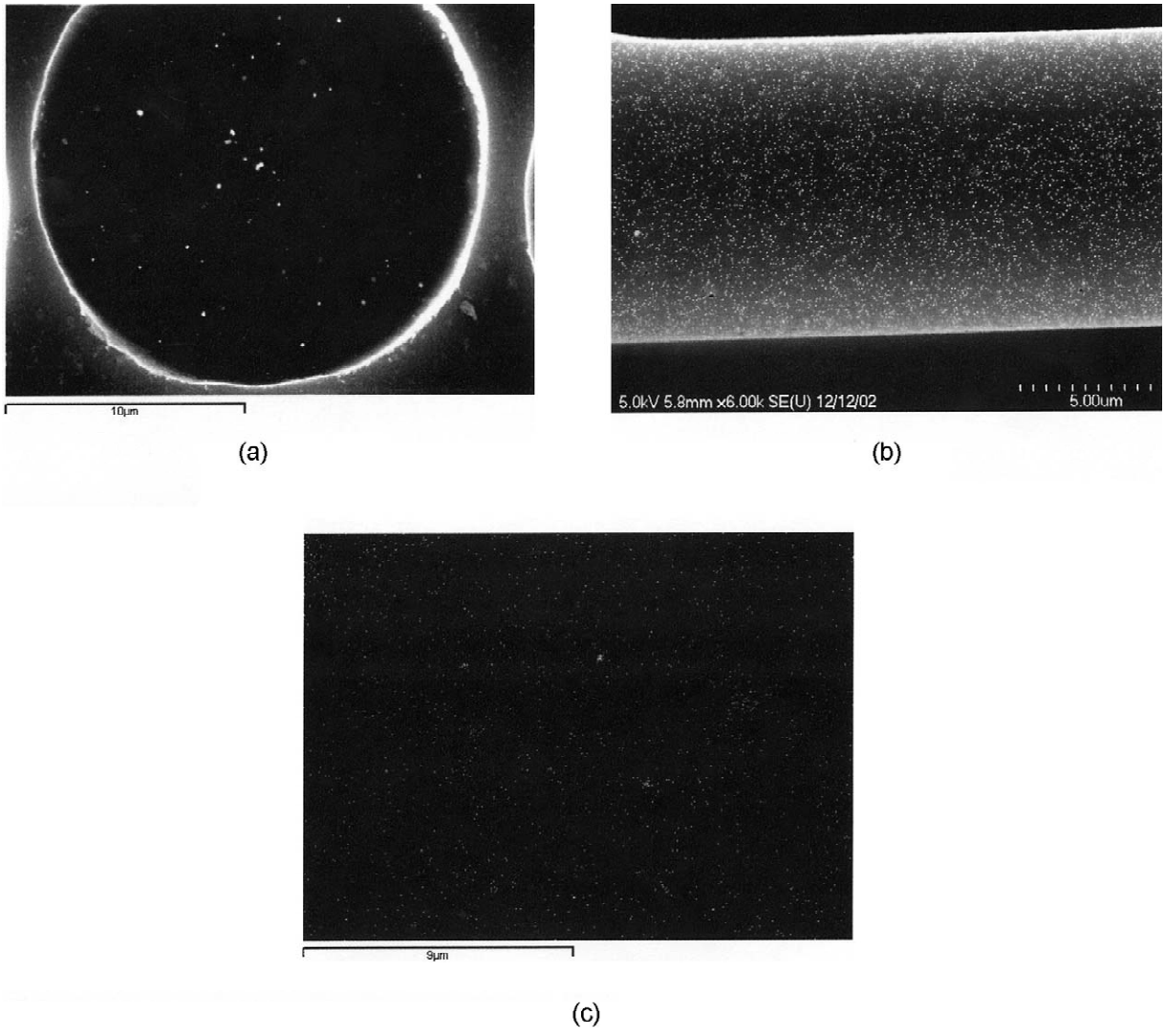

Fig. 2. Distribution of silver particles in mixed carbon fibers. Microscopy observations: (a, b) SEM, and (c) EDS micrographs.

mixtures. Fig. 1 shows typical cross sections of round and trilobal fibers melt spun from the isotropic pitch containing 1 wt.% silver.

The optimum melt spinning temperature for round fibers from the pure Korean pitch samples was found to be 272±1 °C. By comparison, the optimum melt-spinning temperature for round fibers from the Korean pitch containing 1 wt.% silver was 278±2 °C. While fibers can be formed over a range of spinning temperatures, the 'optimum' is defined as the temperature that resulted in the highest yield of fibers. This spinning temperature difference observed for the pure and silver-containing pitches is consistent with that reported by Ryu et al. [3]. They reported that the spinning temperature of silver-containing pitch increased as the silver nitrate content increased. When trilobal fibers were melt spun, the spinning temperatures were about 7 °C lower than those for round fibers spun from the same pitch. This trend was more noticeable for trilobal fibers melt spun from the silver-containing pitch. The spinning yields reported in this work for pitch–$AgNO_3$ mixtures appear to be much better than those reported in a prior study [3]. This is most likely the result of the grinding and mixing procedure used to prepare the pitch–$AgNO_3$ precursor.

As might be expected, the as-spun diameters of the pure and silver-containing carbon fibers decrease upon carbonization (see Table 3). The first letter, K, in the sample notation indicates the pitch source (Korean). The second letter indicates that the pitch used to form the fibers was either a mixture containing 1 wt.% silver (M) or pure and unmixed (U). The third letter represents the fiber cross-sectional shape (R=round). The final number represents the takeup speed used during melt spinning: 1, 286 m/min; 2, 457 m/min; 3, 640 m/min, respectively. During stabilization, oxygen is incorporated into the as-spun fibers. As a result, during this process step the fibers gain about 8–12% in weight. However, carbonization removes this oxygen as well as most of the hydrogen in the stabilized fibers. Thus, the stabilized fibers lose ~30% in weight during this step. This weight loss during carbonization and the corresponding structural collapse causes the decrease in filament diameters.

3.2. Structural properties

SEM and EDS photos of round, silver-containing carbon fibers are shown in Fig. 2. While WDS and EDS are usually considered more accurate for locating heavy elements, the particles could be easily detected as bright spots in the SEM images (see Figs. 2a and b). Each of these analyses showed that the silver particles are uniformly distributed in both the round and trilobal fibers and that the average particle size was less than 100 nm.

As shown in Fig. 3, fibers with similar cross-sectional areas yield comparable burn-off values during activation.

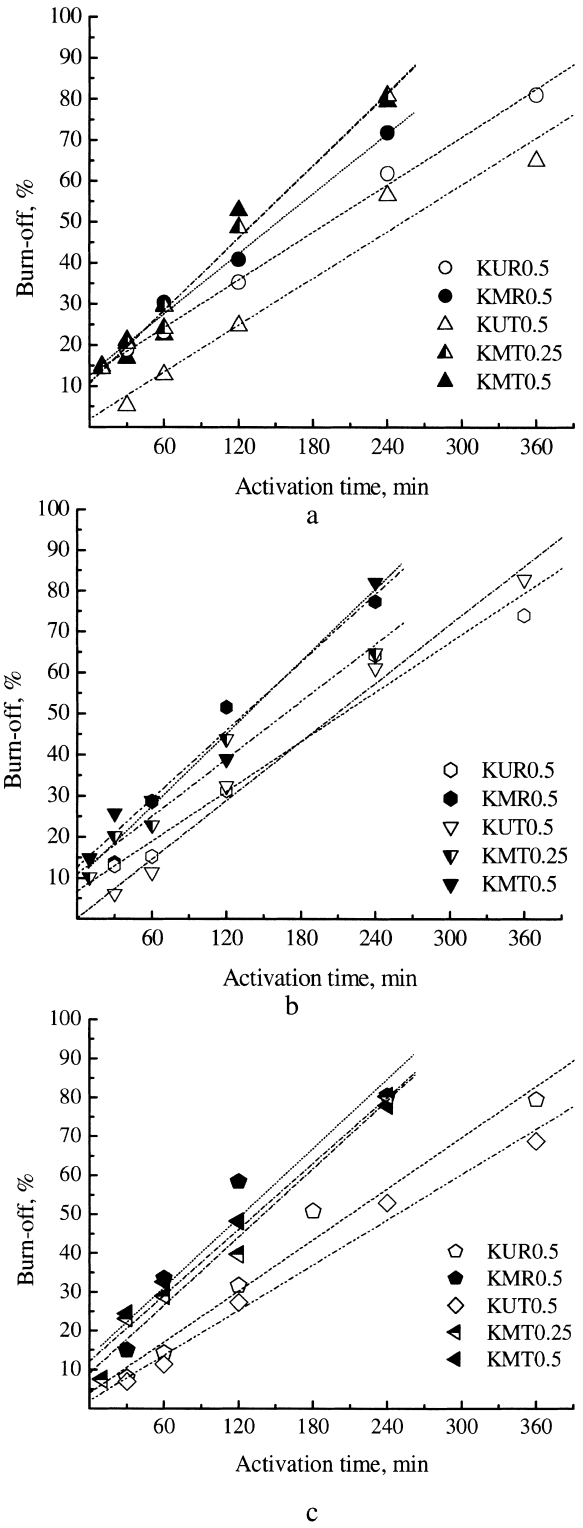

Fig. 3. Weight loss during activation for round and trilobal fibers melt spun from pure isotropic pitch and isotropic pitch containing 1% silver. Activation at 900 °C, CO_2 flow rate 0.25 and 0.5 l/min. Relative takeup speeds: (a) 286 m/min, (b) 457 m/min, (c) 640 m/min, respectively.

In this figure the third letter in the sample notation represents the fiber cross-sectional shape (R=round and T=trilobal), and the final number represents the CO_2 flow rate used during activation (either 0.5 or 0.25 l/min). The overall results indicated that the loss of carbon and weight was highly dependent on the total time of exposure, somewhat dependent on the size of the fiber, and independent of fiber shape. The rate of activation was also found to be independent of CO_2 flow rate.

During activation the CO_2 reacts with the carbon according to the following reaction:

$$C\ (\text{fiber}) + CO_2\ (\text{gas}) \rightarrow 2\ CO\ (\text{gas})$$

This creates pores (micropores) in the fiber as carbon is removed. Figs. 4 and 5 are SEM photos of the surface texture of trilobal and round ACFs produced from isotropic pitch samples containing 1 wt.% silver. As these figures show, both mesopore and macropore openings developed on the surface during activation. Interestingly, the concentration of pores and size of the pore openings appeared to be the same on the outer edge of the trilobal limbs and in the valleys between the limbs. As shown in Figs. 5 and 6, the silver particles appeared to create tunnels behind the particles. Very few of the particles appeared to coalesce into larger particles, even up to 80% burn-off. SEM inspection of cross sections of the ACFs indicated that many silver particles also migrated to the fiber core, creating mesopores and macropores. This was expected, based on the findings reported by Oya et al. [1].

Measurements of the cross-sectional areas of silver-containing ACFs at different degrees of activation show that these areas decrease during the initial stages of activation, but then become relatively constant. This plateau in cross-sectional area appears to correspond with the initial development of mesopores. Perhaps the meso-

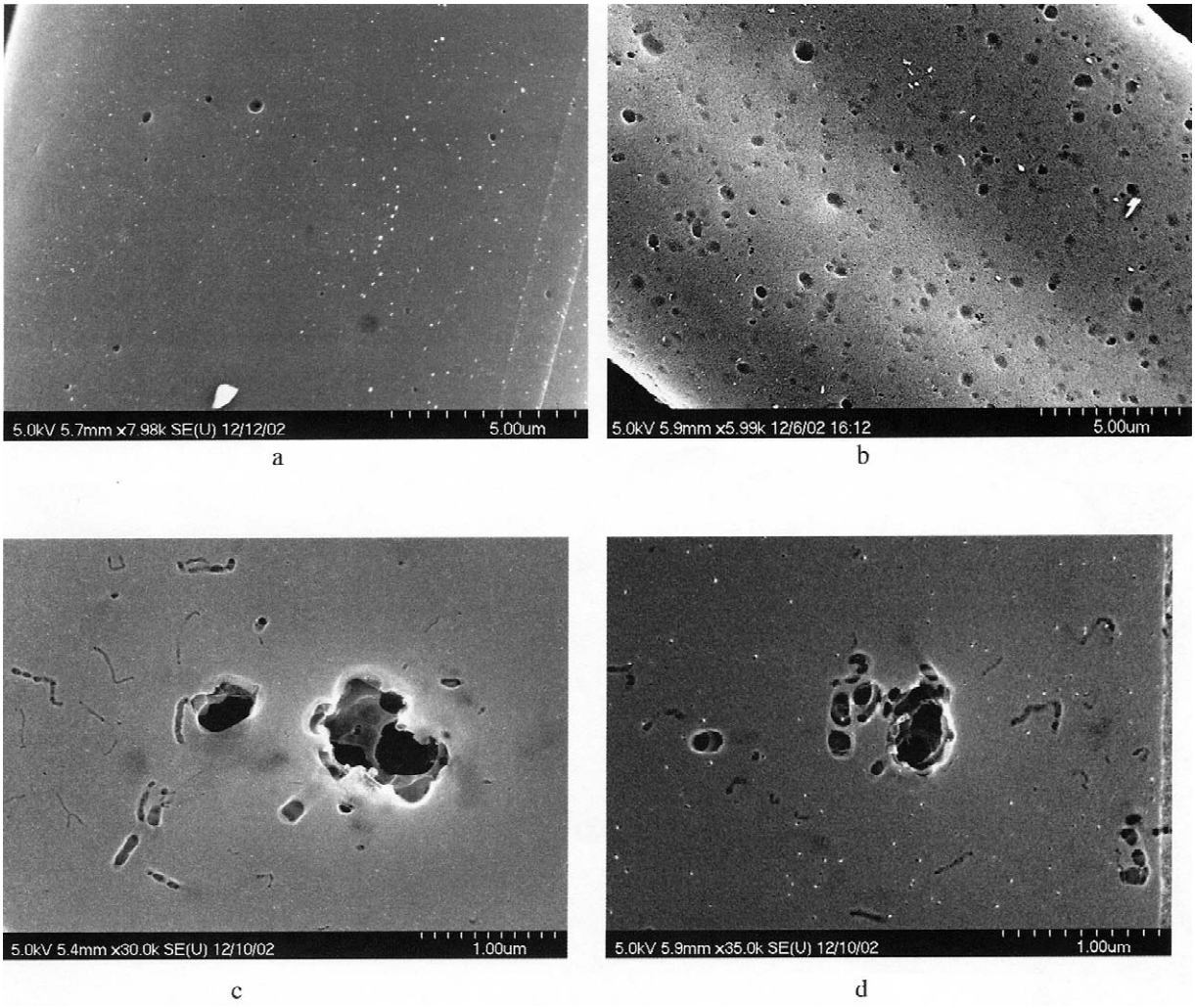

Fig. 4. FE SEM micrographs of surface valleys of trilobal activated carbon fibers at different activation times. (a) 30 min, BO 15%, (b–d) 240 min, BO 80%.

pores increase CO_2 access to the interior of the fiber and allow the product gases to exit more easily.

SEM-BSE analyses of carbon fibers at different degrees of activation (Fig. 7) showed that silver particles remain evenly distributed, in the fiber core and near the fiber surface, during activation. Ryu et al. [3,5] reported that silver particles appear to agglomerate and escape the fiber during activation. Perhaps grinding the silver nitrate into extremely small particles and evenly dispersing these in the precursor pitch avoids these problems. It should be noted that some areas containing larger concentrations of silver particles were observed (Figs. 5c and 7d). This indicates that the current mixing procedure, while improved, is not perfect.

3.3. Determination of specific surface areas and pore characteristics from N_2 adsorption isotherms

Fig. 8 shows the relationship between specific surface area and burn-off for all samples tested. The sample

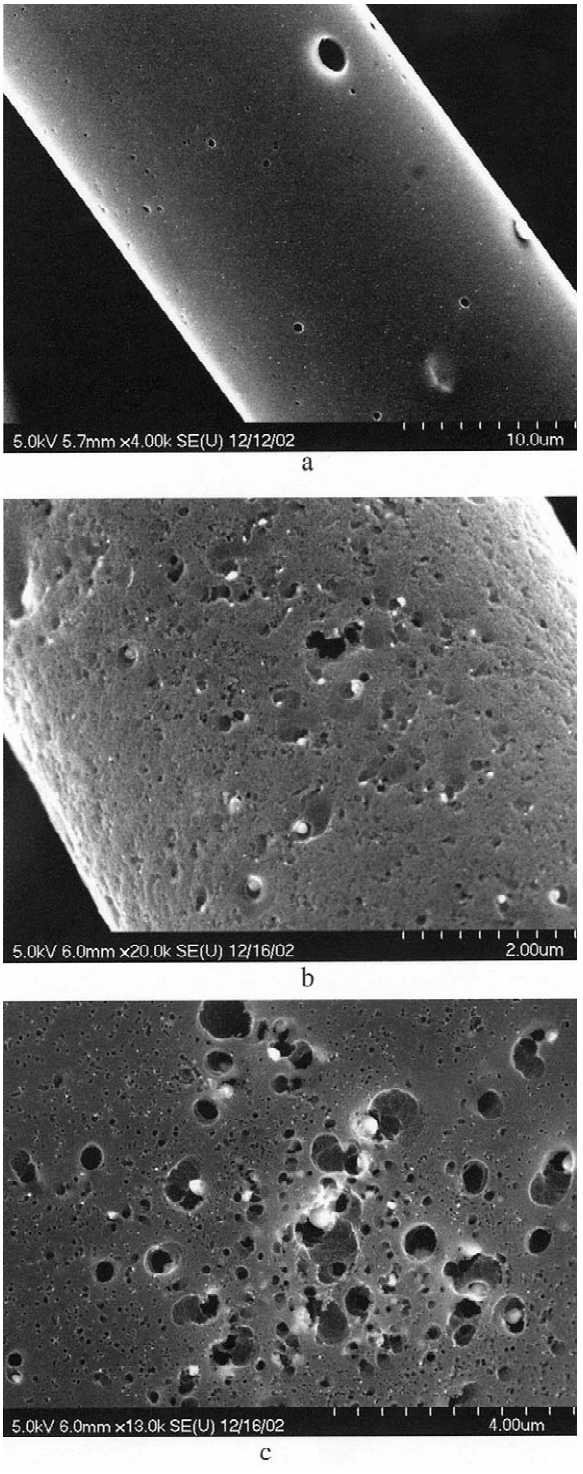

Fig. 5. FE SEM micrographs of surfaces of round carbon fibers after activation. (a) 120 min, BO 58%, (b, c) 240 min, BO 83%.

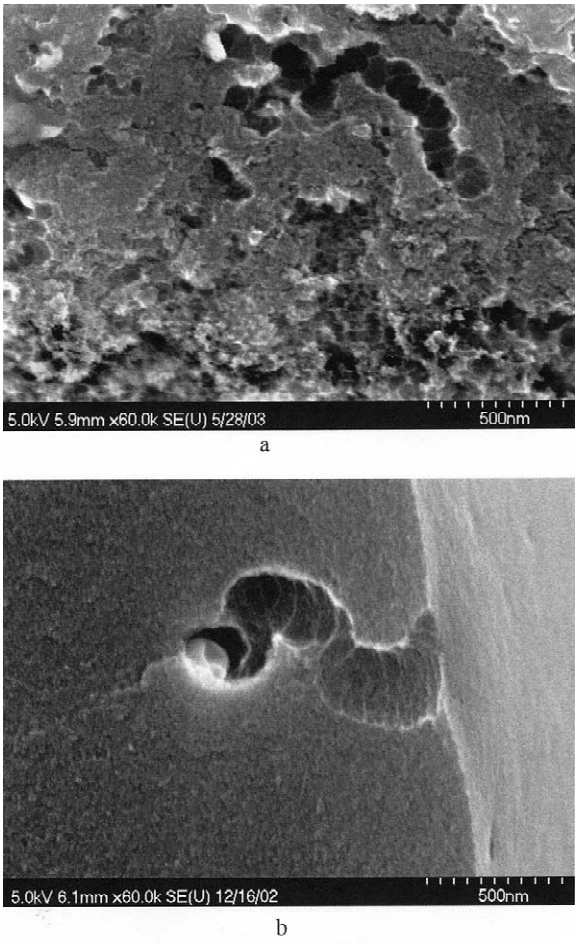

Fig. 6. FE SEM micrographs of fracture surface of (a) trilobal and (b) round carbon fibers activated 240 min, BO 80%.

notation in this figure is identical to that used in Fig. 3. Although there is no absolute correlation between burn-off and specific surface area for all forms of activated carbon, the relationship is commonly used to rank or compare data obtained from similar materials. The BET data confirm that these porous fibers have extremely high specific surface areas. It should be noted that previously reported values for the specific surface areas of metal-containing ACFs were much lower than those found in this study (e.g. 670–830 m^2/g for silver/cobalt-containing ACFs [1], 600–840 m^2/g for cobalt-containing ACFs [11], 540–740 m^2/g [12] and 2000 m^2/g [3] for silver-containing ACFs, 1050–1173 m^2/g for Y and Al-doped ACFs [6,7]). The specific surface areas of the trilobal fibers with equivalent burn-off values were similar to those of the round fibers, when similar values of burn-off are compared.

Fig. 9 shows the representative adsorption isotherms of the ACFs produced in this study. At less than 50% burn-off, almost all adsorption isotherms are type I according to the IUPAC classification [13]. Note that at low values of burn-off the isotherms exhibit a sharp knee followed by a horizontal plateau. This indicates narrow microporosity (i.e. ultramicropores). By contrast, at higher values of burn-off the knee is more rounded, indicating that the pores are widening and microporosity is developing. As can be seen in Fig. 9, at burn-off values greater than about 50%, the knee becomes rounded and the plateau disappears. For these samples, the amount of N_2 adsorbed continues to increase as relative pressure increases. This corresponds to a type IV isotherm and a defining characteristic of mesoporosity. SEM photos of these samples (Figs. 5 and 6) suggest that at 80% burn-off (BO80) larger pores are developed. The adsorption isotherms of unmixed samples with the equivalent degree of burn-off show that this process of mesopore and macropore formation is less pronounced than it is for mixed ACFs.

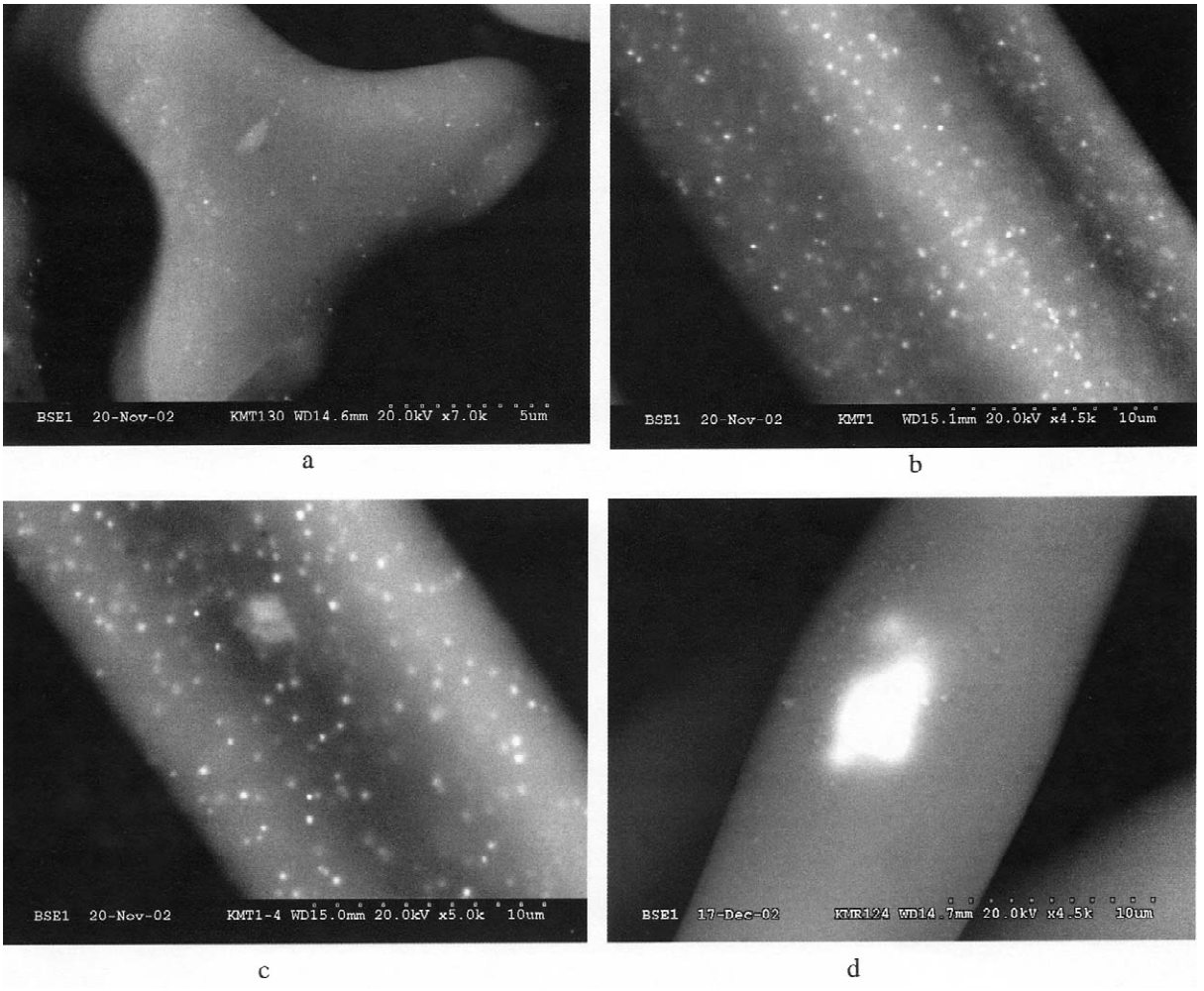

Fig. 7. BSE photos of mixed trilobal fibers activated (a) 30 min, BO 26%, (b) 120 min, BO 40%, (c) 240 min, BO 80%, and (d) of mixed round fibers activated 240 min, BO 80%.

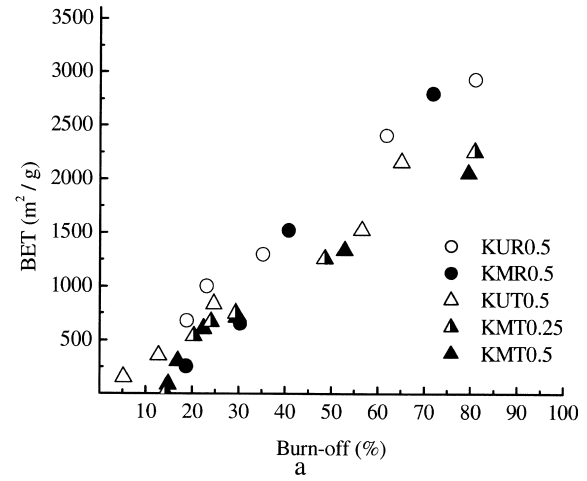

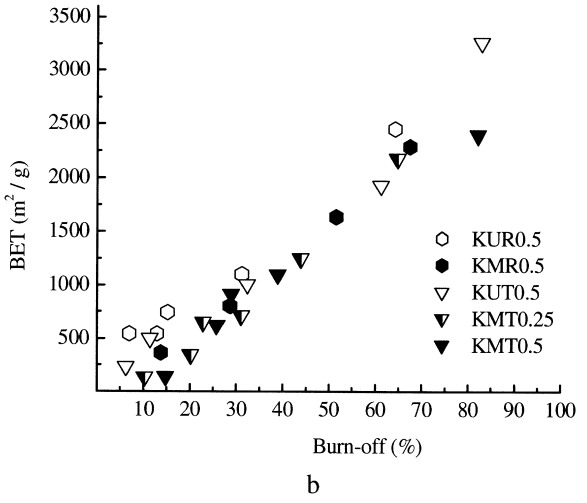

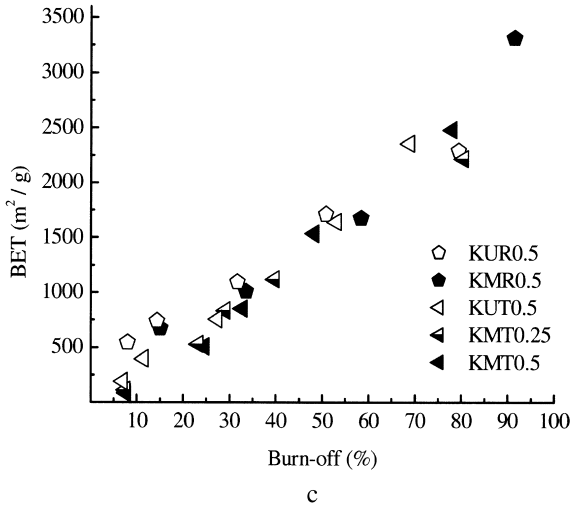

Fig. 8. Specific surface area at various degrees of activation (CO_2 flow rate 0.25 and 0.5 l/min) for round and trilobal fibers melt spun from pure pitch and pitch containing 1% silver nitrate at different takeup speeds. (a) 286 m/min, (b) 457 m/min, (c) 640 m/min.

Adsorption/desorption isotherms for selected high-surface-area ACFs formed from silver-containing pitch and pure pitch are shown in Fig. 10. Here the final numbers in the sample notation represent the activation time (240 = 240 min and 360 = 360 min, respectively). The shape of the adsorption/desorption isotherm for the ACF formed from the pure pitch indicates that the fiber contains mainly micropores. By comparison, isotherms of ACFs formed from the silver-containing pitch (even at shorter activation times) exhibit a hysteresis loop between 0.5 and 0.95 in relative pressure. This suggests that pore-size distribution has extended into the mesopore range.

Although the experiment is extremely time-consuming, valuable information on the relative amount of micropores versus mesopores/macropores can be obtained by measuring N_2 adsorption isotherms over an extended range of relative pressures. Some typical results of this analysis are shown in Fig. 11. The sample notation in this figure is the same as that used in Fig. 10. The amount of adsorbed nitrogen on the fibers formed from silver-containing pitch was found to be smaller than that for similar fibers formed from pure pitch at very low relative pressure ($<10^{-4}$). Adsorption at these pressures is normally attributed to the filling of ultramicropores and micropores [14]. However, at moderate relative pressures (10^{-4}–10^{-2}) the amount of N_2 adsorption for the silver-containing ACFs was greater than that for the pure ACFs. Adsorption in this range of relative pressures can be attributed to monolayer formation on the surfaces of wider micropores such as supermicropores and small mesopores. At high relative pressure (between 10^{-2} and 1.0) the silver-containing ACFs adsorbed noticeably more N_2 than the pure ACFs (even at shorter activation times). This indicates that the silver-containing ACFs contain an appreciable amount of mesopores and macropores, in addition to micropores.

As previously mentioned, nitrogen isotherms were analyzed by the BET method to obtain the total surface area. The Barrett–Joyner–Halenda (BJH) method was applied to the same isotherms to estimate the mesopore surface area and the mesopore volume. The ratio of these two surface areas is a measure of mesopore percentage. Typical results are shown in Table 4. This table and Fig. 12 show that mesopore volume and mesopore ratio increase with activation for round and trilobal ACFs. This trend is more pronounced for the silver-containing ACFs.

Apparently, in this case silver particles do not block pores during activation, as was reported in Ref. [15]. Instead, they appear to have a catalytic effect on the development of the surface area during activation. When equivalent burn-off values are compared, the specific surface areas of the mixed ACFs are similar to those of pure ACFs. However, mixed samples appear to contain a higher degree of mesoporosity. Moreover, mixed fibers require much shorter activation times to develop a given specific surface area.

Based on these results, the adsorption characteristics of

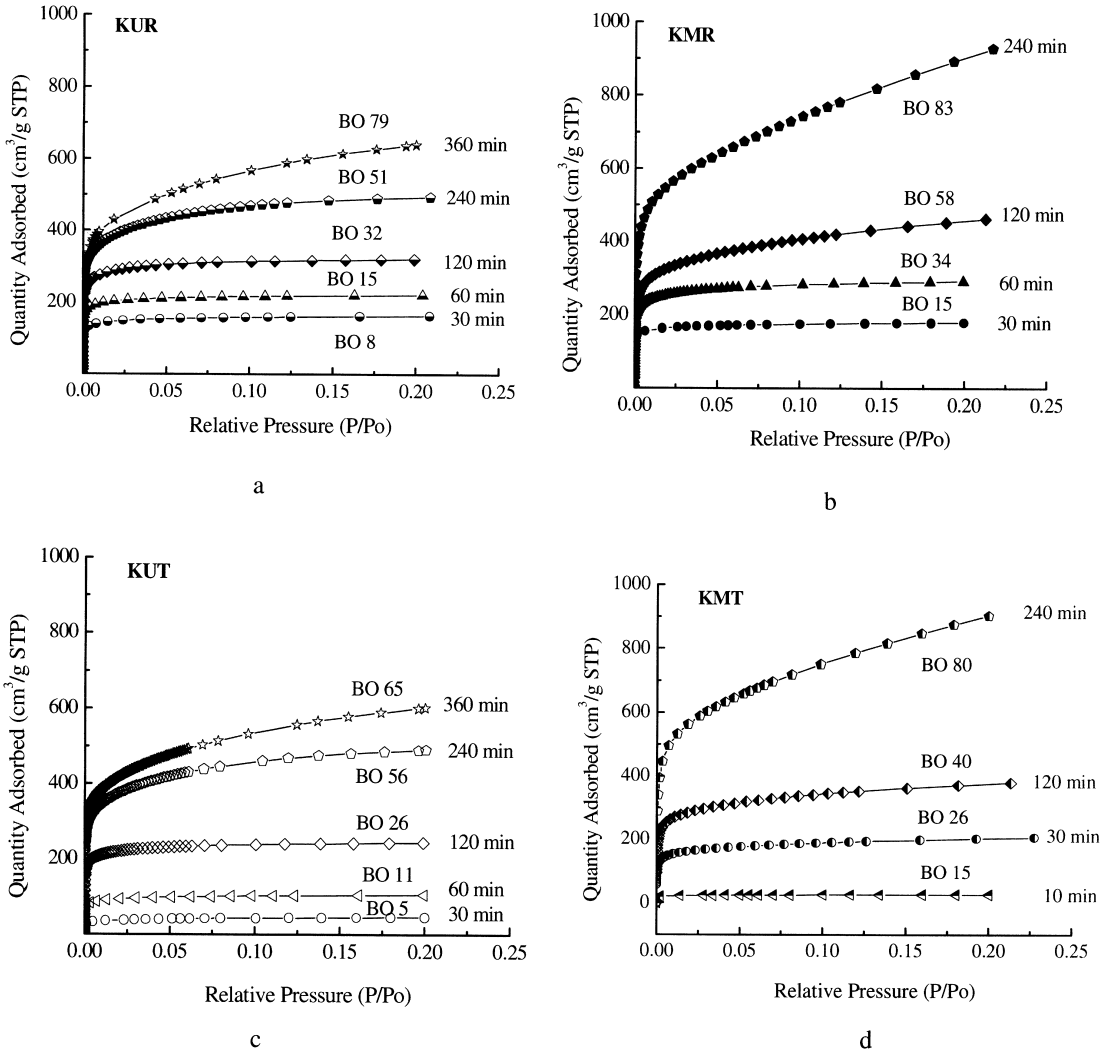

Fig. 9. Nitrogen adsorption isotherms for round and trilobal carbon fibers at different degrees of burn-off (BO). (a) KUR, (b) KMR, (c) KUT, (d) KMT.

Table 4
Pore structure analysis for selected ACFs activated at 900 °C and a CO_2 flow rate of 0.5 l/min

Sample	Activation time (min)	Burn-off (%)	V_{total} (cm^3/g)	V_{meso} (cm^3/g)	Mesopore ratio (%)
KMR	30	15	0.34	0.02	5.1
KMR	60	34	0.42	0.05	9.4
KMR	120	58	1.31	0.32	17.9
KMR	240	80	1.44	0.82	42.8
KUR	120	31	0.49	0.05	7.8
KUR	240	51	0.82	0.14	12.8
KUR	360	79	1.26	0.55	34.7
KMT	240	78	0.99	0.47	38.0
KUT	360	65	1.07	0.39	27.4

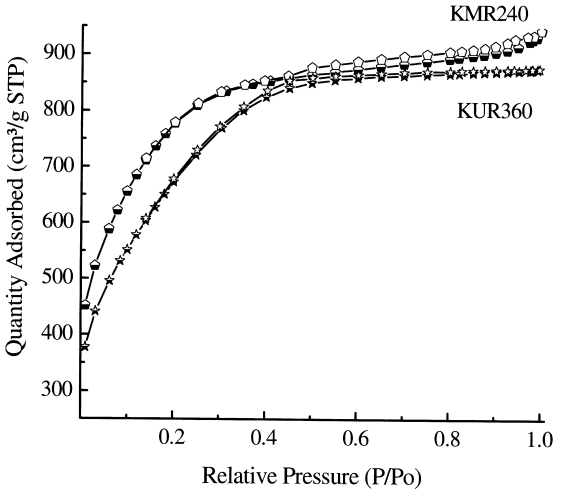

a

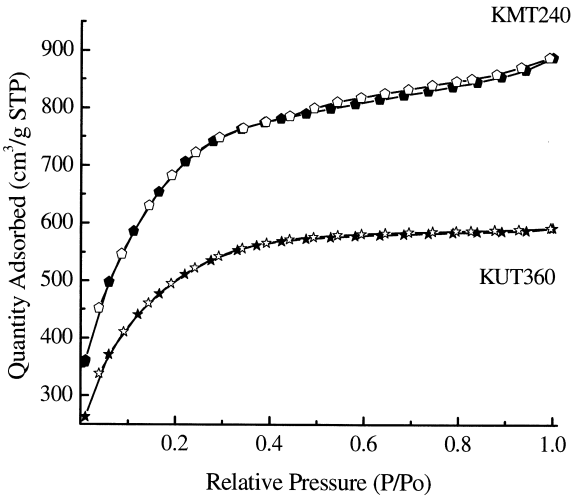

b

Fig. 10. Typical nitrogen adsorption isotherms for unmixed and mixed carbon fibers after different activation times. (a) KUR = 360 min, KMR = 240 min, (b) KUT = 360 min, KMT = 240 min.

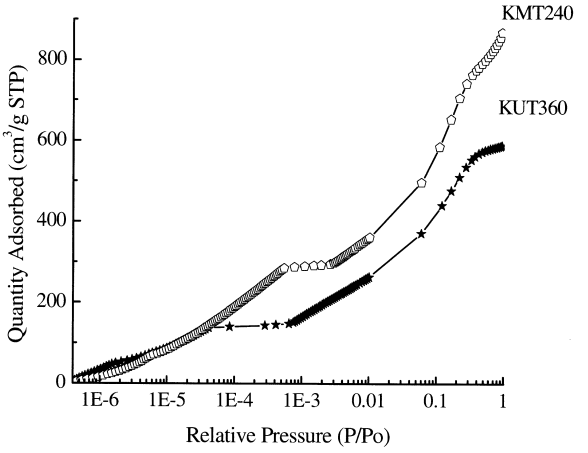

Fig. 11. Low-pressure adsorption isotherms plotted on the logarithmic scale for ACFs after different activation times. KUT = 240 min, KMT = 360 min.

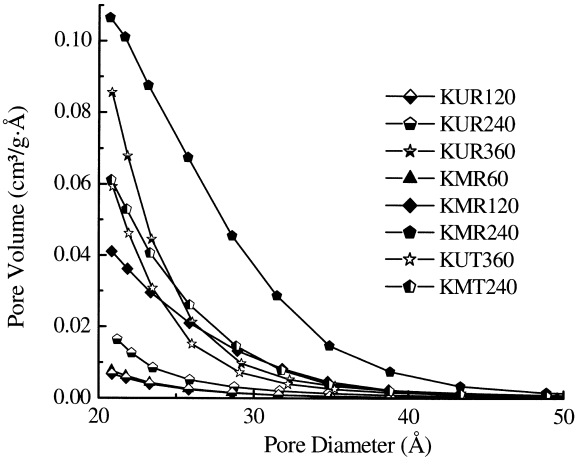

Fig. 12. Mesopore size distribution curves for round and trilobal ACFs after different activation times.

trilobal fibers are equal to those of similarly sized round fibers. However, past studies indicate that trilobal fibers offer the additional advantages of increased bed porosity and, thus, lower pressure drop in filter applications [16].

4. Conclusions

Round and trilobal fibers can be easily spun from pure pitch precursors and mixtures containing 1 wt.% of silver. The mixing procedure evenly distributed the silver nitrate in the isotropic pitch precursor. Silver particle distribution remained relatively uniform throughout the fibers after activation, even at high burn-off values (BO80). Silver particles appear to catalyze the activation process near their surface. This widens the micropores and creates mesopores, as well as macropores. The adsorption characteristics of trilobal ACFs were found to be equal to those of round fibers, when fibers of similar cross-sectional areas were compared.

Acknowledgements

Partial support was provided by the ERC Program of the National Science Foundation under Award Number EEC-9731680. Funding was also provided by Philip Morris Inc.

The authors would like to thank Dr. Wei of CononoPhillips for conducting some of the SEM, EDS and WDS analyses.

References

[1] Oya A, Yoshida S, Alcaniz-Monge J, Linares-Solano A. Preparation and properties of an antibacterial activated carbon fiber containing mesopores. Carbon 1996;34(1):53–7.
[2] Ryu SK, Kim SY, Gallego NC, Edie DD. Preparation and characterization of silver-containing activated carbon fibers. In: Extended abstracts, Eurocarbon 98, Strasbourg, France; 1998, pp. 595–6.
[3] Ryu SK, Kim SY, Gallego N, Edie DD. Physical properties of silver-containing activated pitch-based carbon fibers. Carbon 1999;37(10):1619–25.
[4] Yim KS, Ryu SK, Edie DD. Characterization of metal(Ag, Cu, Co)-containing pitch-based activated carbon fibers. In: Extended abstracts, International Conference on Carbon, Beijing, China; 2002.
[5] Ryu SK, Kim SY, Li ZJ, Jaroniec M. Characterization of silver-containing pitch-based activated carbon fibers. J Colloid Interface Sci 1999;220:157–62.
[6] Ikeuchi M, Kojima S. Extremely large mesoporous carbon fibers synthesized by the addition of rare earth metal complexes and their unique adsorption behaviors. Adv Mater 1997;9:55–8.
[7] El-Merraoui M, Tamai H, Yasuda H, Kanata T, Mondori J, Nadai K et al. Pore structure of activated carbon fibers from organometallics/pitch composites by nitrogen adsorption. Carbon 1998;36(12):1769–76.
[8] Beauharnois ME, Edie DD, Thies MC. Carbon fibers from mixtures of AR and supercritically extracted mesophases. Carbon 2001;39:2101–11.
[9] Sheikh SY. The effect of mesophase composition on rheology and final fiber properties. Clemson, SC: Clemson University; 1999, MS thesis.
[10] Lin SS. Oxidative stabilization in production of pitch based carbon fibers. J Soc Adv Mater Process Eng 1991;27:9–14.
[11] Oya A, Yoshida S, Alcaniz-Monge J, Linares-Solano A. Formation of mesopores in phenolic resin-derived carbon fiber by catalytic activation using cobalt. Carbon 1995;33(8):1085–90.
[12] Oya A, Wakahara T, Yoshida S. Preparation of pitch-based antibacterial activated carbon fibers. Carbon 1993;31(8):1243–7.
[13] Gregg SJ, Sing KSW. In: 2nd ed, Adsorption, surface area and porosity, London: Academic Press; 1982, p. 242.
[14] Kakei K, Ozeki S, Suzuki T, Kaneko K. Multi-stage micropore filling mechanism of nitrogen on microporous and micrographitic carbons. J Chem Soc Faraday Trans 1990;86(2):371–6.
[15] Wang YL, Wan YZ, Dong XH, Cheng GX, Tao HM, Wen TY. Preparation and characterization of antibacterial viscose-based activated carbon fiber supporting silver. Carbon 1998;36(11):1567–71.
[16] Rasmussen G, Renfro LW. Fiber distribution and pressure drop in cellulose acetate cigarette tow cigarette filters. In: Aerosols formation and reactivity, Proceedings of the Second International Aerosol Conference, Berlin, Germany, September 22, Oxford: Pergamon Press; 1986, pp. 682–5.